Validation Status of the OMI Ozone Profile Product OMO3PR

		Date	Signature
Author:	J.P. Veefkind M. Kroon J.F de Haan		
Checked:			
Approved:			
Archive:			

Distribution list:

OMI Science team
Pieternel Levelt   KNMI
PK Bhartia   NASA/GSFC

KNMI
Roeland van Oss   KNMI

Agencies
Harry Förster   NIVR
Johanna Tamminen   FMI

EOS-Aura project

Industry

Change status:

Issue	Date	Comments	Affected pages
Issue 1, draft	24-10-2008	First draft	All
Issue 1.5, draft	25-06-2009	Update after revision algorithm	All

1   Introduction

This document describes the validation status of the ozone profile product (OMO3PR) of June 2009. The EOS Aura platform provides several co-located measurements of ozone that are used in this document. The Microwave Limb Sounder (MLS) makes accurate measurements of the ozone profile down to the lower stratosphere [Froidevaux et al., 2008]. An inter-comparison with this validated MLS product is a very efficient approach to assess the accuracy of the OMI ozone profile product.

2   OMO3PR Algorithm Description

The retrieval algorithm is based on optimal estimation (Rodgers [2000]) with climatological a-priori information. Basically the amount of ozone in each atmospheric layer is adjusted such that the difference between the modelled and measured sun-normalized radiance is minimal. As the information content in the measured spectrum is not sufficient to determine the ozone amount for all layers, a side-constraint is used by demanding that the retrieved profile does not differ too much from the climatological average. The measurements are taken from the UV1 channel (270 nm – 310 nm) and the first part of the UV2 channel (310 nm – 330 nm). Here two UV2 pixels are combined to obtain the spectrum of a pixel that corresponds to one pixel in the UV1 channel. Small differences in alignment are dealt with by assuming that the cloud cover and the surface albedo for the two channels can be different.

 The algorithm uses the newly developed LABOS radiative transfer model, which replaces the 6 stream Lidort-a model that is currently used for GOME and GOME 2. LABOS includes an approximate treatment of rotational Raman scattering, pseudo spherical correction for direct sunlight, and corrections for the initial assumption that the atmospheric layers are homogeneous. Polarization is ignored in the radiative transfer calculations and a look-up table with polarization correction factors is used to compensate for this. Forward calculations are performed in the wavelength range 267 – 332 nm on a sufficiently fine wavelength grid such that after interpolation the error in the reflectance is less than 0.2% for any wavelength considered. This facilitates convolutions with rotational Raman lines and convolutions with the OMI slit function after multiplication with a high-resolution solar spectrum. A Chebyshev expansion combined with a LUT is used to perform the convolution with the OMI slit function in an efficient manner.

The surface below the atmosphere is assumed to be a Lambertian reflector and has an initial value taken from a surface albedo climatology. The surface albedo for the UV1 and UV2 channels is fitted separately in the algorithm. In version 1.1.0 the surface albedo is a quadratic polynomial in the wavelength for each channel. The cloud fraction is taken from the OMCLDO2 product. If the cloud fraction exceeds a threshold (currently 0.2???) the cloud albedo instead of the surface albedo is fitted. Similar as for the surface albedo, the cloud albedo is a quadratic polynomial in the wavelength and separate fits occur for the two channels. In the previous version (1.0.5) the cloud fraction was fitted, but in the current version (1.1.0) the cloud albedo is fitted, enabling us to deal with optically thick bright clouds that have an albedo larger than 0.8.

In the current version stray light is fitted separately for the two channels. A quadratic polynomial in the wavelength is used for stray light in each channel. This lads to a substantial reduction of Fraunhofer features in the residue of the fit and reduces oscillations in the retrieved profiles when they a compared with MLS profiles.

The Gauss-Newton method, used in version 1.05 for iteratively solving the profile, is replaced by a modified Levenberg-Marquardt method in order to improve convergence when the a-priori differs strongly from the true profile. This greatly improves the convergence during ozone hole conditions.

The measurement errors used in optimal estimation are taken from the level 1b product.

The Fortuin-Kelder [1998] climatology, used in version 1.05 as a-priori, is replaced by a climatology based on McPeters and Labow for the a-priori profiles (see Specific Realese Info for more details). Optimal estimation is started with the a-priori and a maximum of 7 iteration steps is allowed for convergence. The current default is

that the convergence of the state vector is tested according to Eq. (5.28) in Rogers [2000], with a threshold of 1.0.

3   Characteristics of OMO3PR Data

In this section the characteristics of the OMO3PR retrievals are discussed in terms of the averaging kernel and the errors.

The averaging kernel describes the sensitivity of the retrieval at various altitudes. Figure 1 and Figure 2 show the averaging kernel matrix for a typical OMO3PR retrieval. Ideally, the averaging kernel should have values of unity on the diagonal and zero for the off-diagonals. As can be seen in Figure 1 and Figure 2, in the stratosphere, at pressures less than approximately 100 hPa, the averaging kernels peak at the right altitude and are sufficiently sharp. Some of the stratospheric averaging kernels do have significant negative contributions at other altitudes, for example Layer 6 in Figure 2. In the troposphere (the lowest 3-4 layers in Figure 1 and Figure 2) the averaging kernels are very broad, which shows that there is not much vertical information present. In fact, typically one piece of information on the troposphere is available. Although the sensitivity of the retrievals decreases in the lower troposphere, some information is obtained on the lowest layers. In the upper troposphere and lower stratosphere, the retrievals are not very sensitive, as can be seen by the low values of the averaging kernels in the layers 12 to 14.

The averaging kernels as shown in Figure 1 and Figure 2 are confirmed by retrieval simulation studies. The low sensitivity in the upper troposphere and lower troposphere as well as the limited information in the troposphere are due to the limited information in the UV spectral region as caused by the low surface albedo and large stratospheric ozone amount as compared to the troposphere.
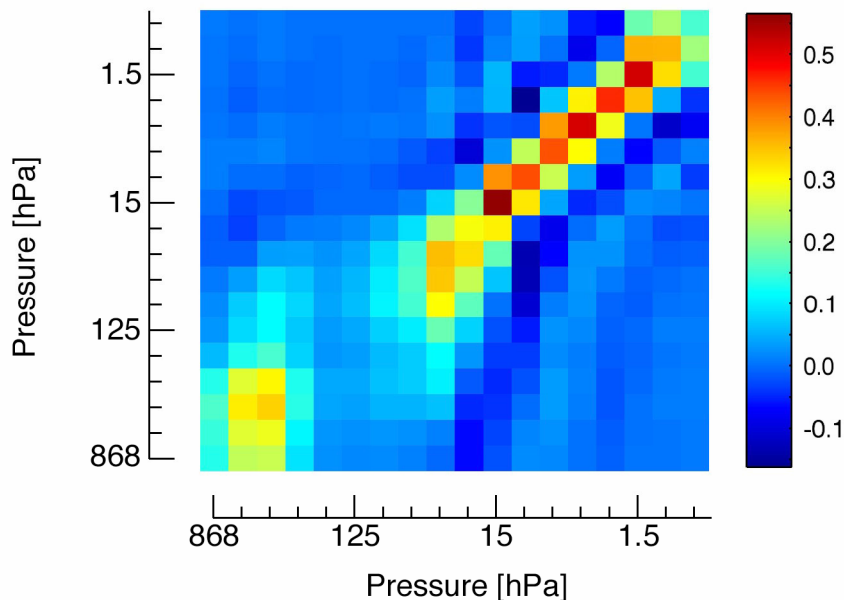

Figure 1. The averaging kernel matrix for a typical OMO3PR ozone profile retrieval. The averaging kernel is expressed in units of ln(VMR).
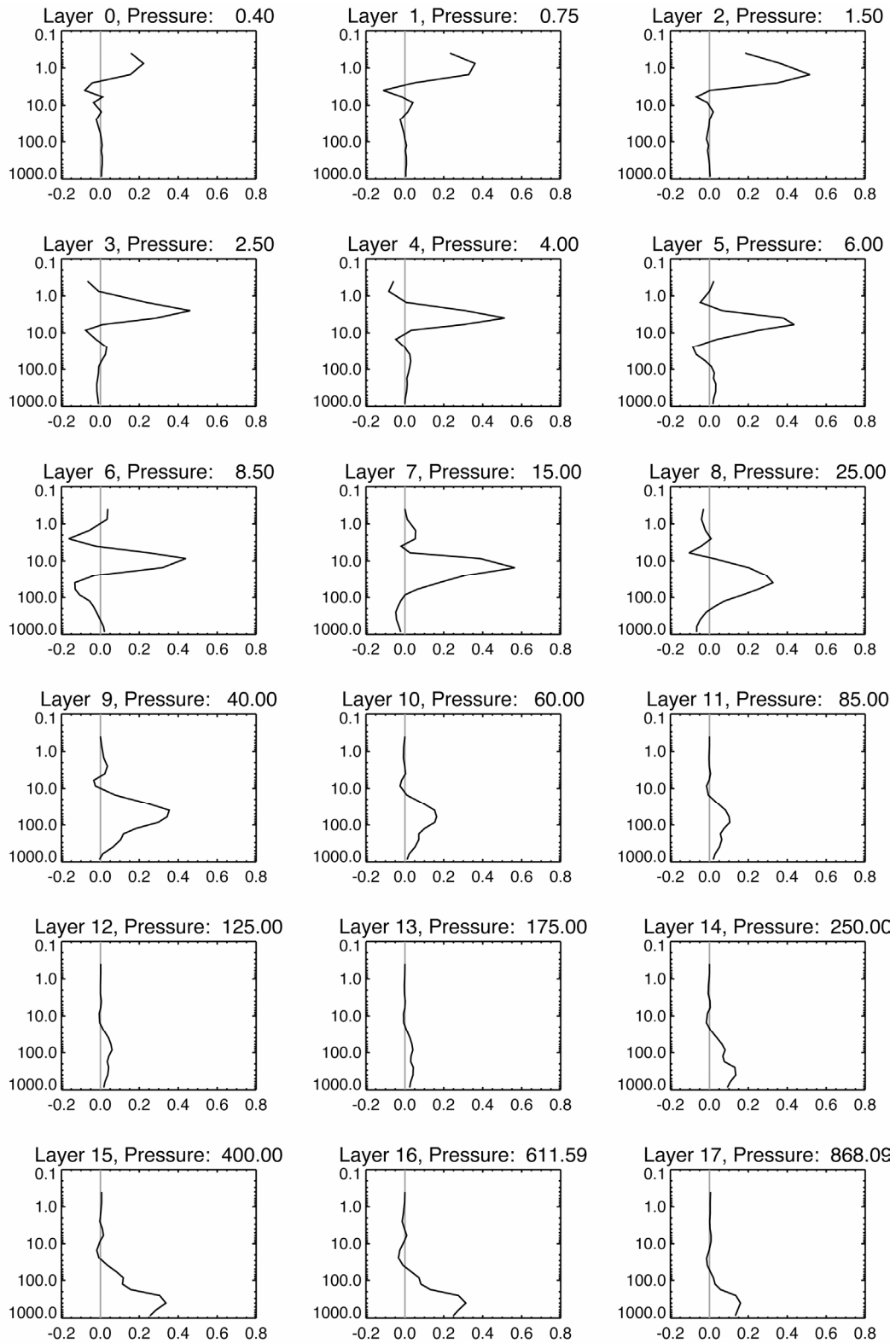
Figure 2. Averaging kernels for the retrieval layers. The information is the same as in Figure 1, presented in a different way. On the y-axes the pressure in hPa is plotted, on the x-axis the averaging kernel.
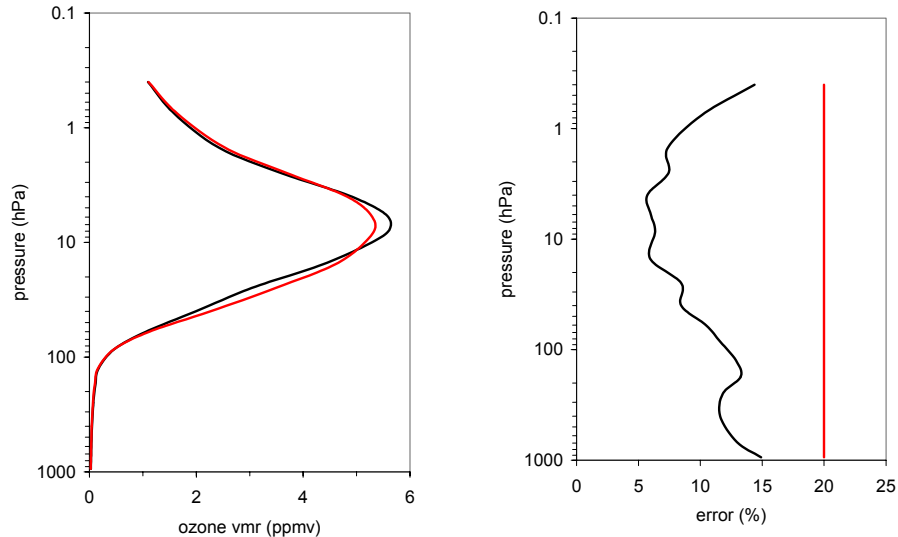
Figure 3. Left panel: Example of the retrieved (black) and a-priori (red) ozone profile. Right panel: retrieval error (black) and a-priori error (red).

As discussed in section 2, the OMO3PR retrieval is based on optimal estimation and uses a-priori information to constraint the result. Figure 3 shows an example of the a-prior and retrieved profile and errors. Although the retrieved profile may not differ too much from the a-priori profile, it is very important to also look into the reduction of the error between the a-priori and the retrieval. If the retrieval is almost identical to the a-priori, but the total retrieval errors have decreased by a factor of two as compared the a priori error, we are much more certain about the ozone profile after the retrieval than before.

4   Comparisons with MLS

The MLS/Aura retrievals have a vertical resolution of approximately 3 km in the stratosphere. The horizontal resolution is of the order 200 km. The estimated error in the retrieved ozone values for the layers at pressures less than 300 hPa is typically 5-10%, with higher values in the lower stratosphere [Froidevaux et al., 2008]. Because OMI and MLS are both on the Aura satellite, there are many co-located measurements. The OMI across track pixel that is closest to the MLS footprint is pixel number 17 out of 29 (zero based) in the UV-1. This is slightly east of the nadir pixel on the dayside of the orbit. Because of the large number of co-locations and the good accuracy in the stratosphere, the MLS data are excellent for comparisons with the OMI profiles.

We have compared the OMI and MLS profiles for a period of nearly one year (week 11, 2005 - week 5, 2006). OMI profiles have been compared to MLS profiles, using only MLS "good quality" retrievals. The co-location criteria used were 100 km between the centres of the ground pixels and within 10 minutes of each other to avoid selection of different orbits for OMI and MLS. In order to compare the OMI and MLS profiles, the OMI data have been converted to volume mixing ratios and the MLS data have been re-sampled on the OMI vertical grid. Examples of OMI-MLS comparisons for individual profiles are shown in Figure 4a and 4b. The green line is the OMI a-priori profile, the black line is the MLS profile on the MLS grid, the blue line is the MLS profile mapped to the OMI grid (taking into account the OMI averaging kernel), and the red line is the OMI profile.
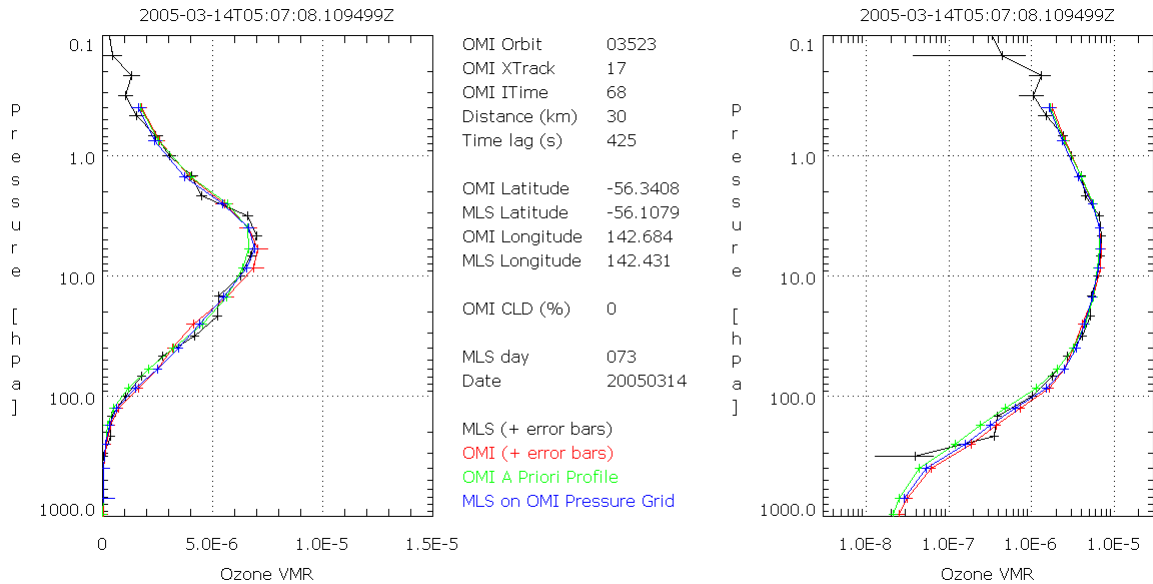
Figure 4a. Example of a OMI-MLS profile comparison for one individual profile. The right panel is the same as the left, except for the logarithmic scale.
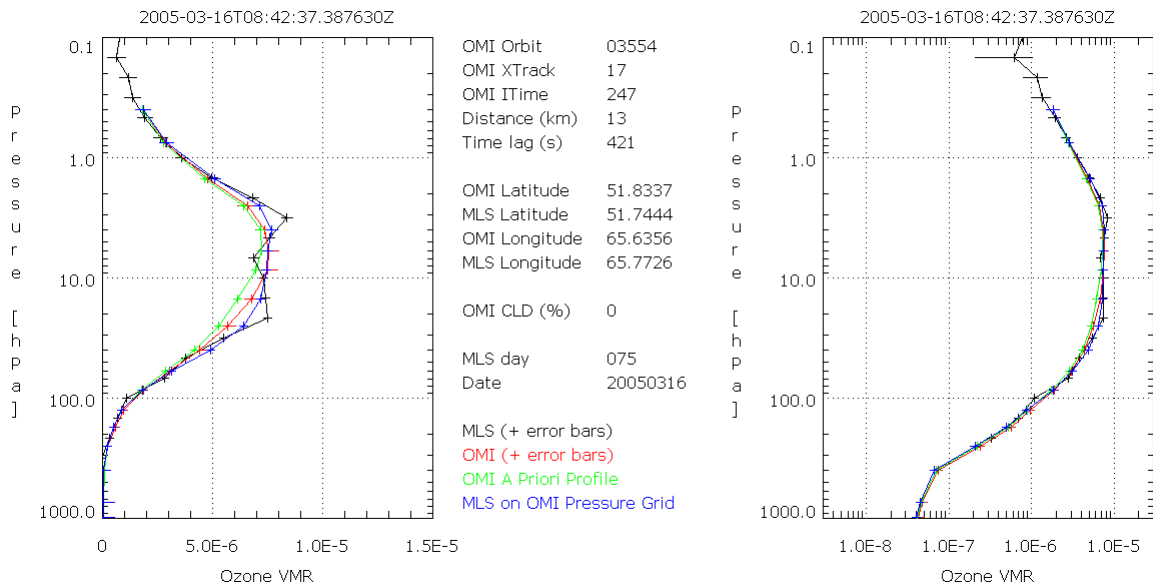

Figure 4b. Same as Figure 4a, but for a location in the northern hemisphere.

Comparisons for three typical profiles, a tropical profile, a mid-latitude profile, and a profile in the ozone hole where part of the ozone has vanished is shown in Figure 5. It shows that the differences between the OMI and MLS profiles are much smaller than the differences between these typical profiles.
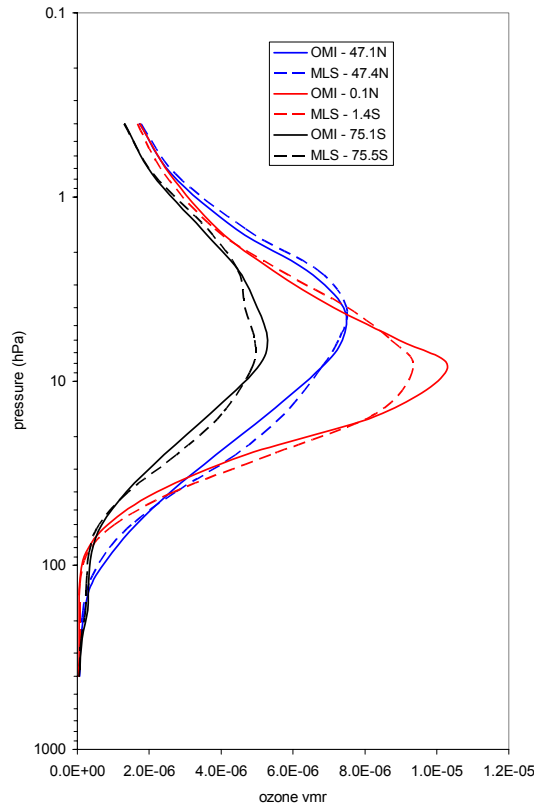
Figure 5. Comparison of retrieved profiles for three typical profiles: tropical (red), mid-latitude (blue), and a profile in the ozone hole with a reduced amount of ozone (black).

Average differences are shown in Figure 6 for different latitude bands. This figure clearly shows that in the OMI profiles compared to MLS there remain oscillations. Oscillations like this, but with larger amplitude were present before stray light was fitted. From simulations it is known that oscillations larger these are expected if stray light is not taken into account, if a spectral slope in the surface albedo is ignored, if rotational Raman scattering is not taken into account, and if the absorption cross section as function of wavelength and temperature is inaccurate. The remaining oscillations might be due to a combination of such effects. For example, we expect oscillation up to about 6% due to the approximation used for Rotational Raman scattering.

Figure 6 also shows larger differences for the southern hemisphere than for the northern hemisphere. Also, the bright green line (75N – 90N) shows a behaviour that differs from the other curves, in particular for pressure < 10 hPa. These differences remain to be investigated.
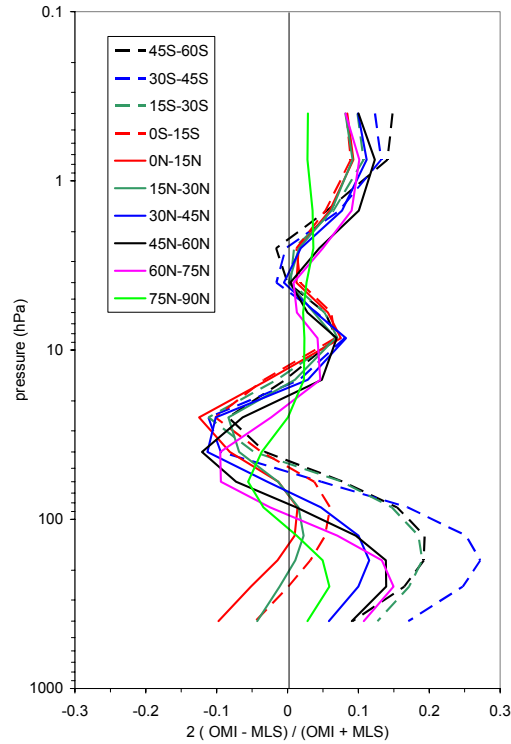
Figure 6. Average relative differences between ozone profile retrieved from OMI and MLS for week 30 2005 (OMI orbits 5428 – 5529). Results are given for different latitude bands and solid lines are for the northern hemisphere while dashed lines are for the southern hemisphere. For each latitude band about 2000 co-locations were used, except for 45S-60S where 681 co-locations were used.
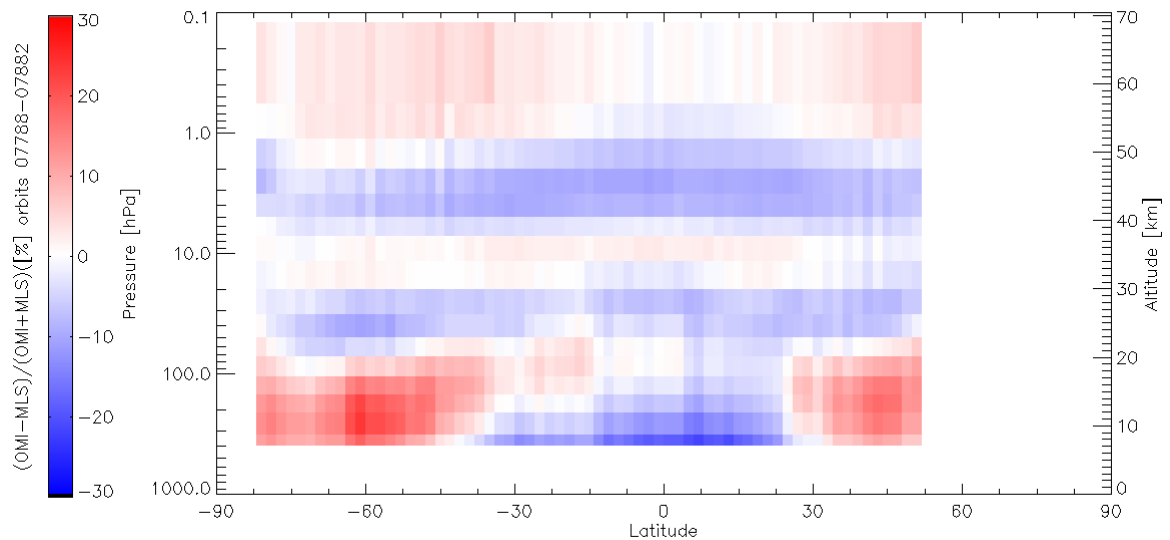

Figure 7a. OMI-MLS for all latitude bands for retrievals for week 01 of 2006.
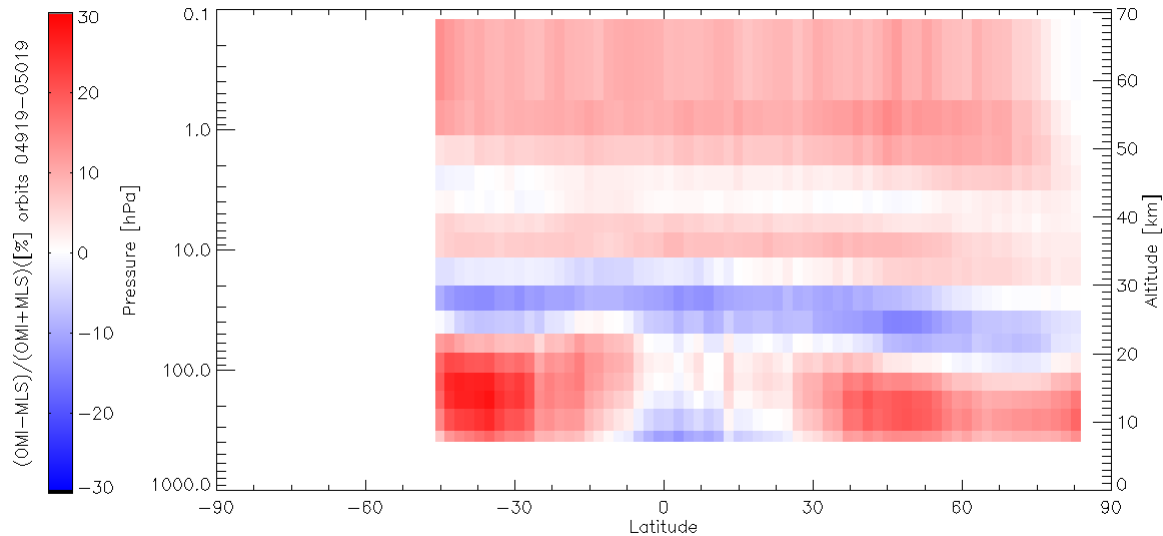
Figure 7b. Same as Fig 7a, but for week 25 of 2005.

Figures 7a and 7b show the mean differences between the retrieved ozone profiles for OMI and MLS for week 1 of 2006 and week 25 of 2005. The overall pattern is about the same, but these are differences. For example, in week 25 the differences are small around 3 hPa, whereas the differences are small around 10 hPa in week 1. Further, for pressure below 1 hPa the differences are larger in week 25 than in week 1.

5   Conclusions

In this report comparisons are presented of the OMI ozone profile product (OMO3PR) with the MLS ozone profile data. Also, the characteristics of the OMO3PR ozone profile product are discussed.

Overall the OMO3PR optimal estimation results are as expected from simulated results. The averaging kernels are well behaved in the stratosphere. In the troposphere the averaging kernels are broad and approximately one piece of independent information is available for the entire troposphere. In the upper troposphere and lower stratosphere little profile information is contained in the UV spectrum.

Comparison with MLS for the pressure range up to 400 hPa show that there remain oscillations in the retrieved profile, but with are reduced amplitude compared to previous versions of the algorithm. Except for pressures larger than 70 hPa at mid-latitudes the differences tend to be 10% or less. At mid-latitudes for pressures >70 hPa the difference is of the order of 20% - 25%. The differences were about a factor of 2-3 larger in the previous versions of the OMI algorithm. The main improvement is due to the fitting of stray light in the new version. However, this correction for stray light is not perfect. Other imperfections of the model used for the retrieval may also contribute to the remaining oscillations, such as inaccuracies in the absorption cross section of ozone, only approximately accounting for the Ring effect, Remaining instrument errors such a wavelength dependent multiplicative offset are not taken into account and might also contribute to the observed differences. Finally, differences in the a-priori information (profile, error covariance matrix) might also have a significant impact on the results of the comparison.

The results presented in this document focus on the stratospheric profile and the total column. The tropospheric sub-column has not been evaluated, because MLS does not give reliable values for pressures larger than about 200 hPa.

6   References

Froidevaux et al., Validation of Aura Microwave Limb Sounder stratospheric ozone measurements, JGR, Vol. 113, D15S20, doi:10.1029/2007JD008771, 2008.

Rodgers, C. 2000. Inverse Methods for Atmospheric Sounding: Theory and Practice. World Scientific Publishing Co. River Edge, NJ.

Appendix A: Calculating tropospheric and stratospheric ozone columns and corresponding diagnostic information

It is assumed that the pressure level of the tropopause, p_T, is known from external sources. In order to calculate the tropospheric and stratospheric columns a summation array is constructed, $\mathbf{W}$, such that $\mathbf{Wx} = \mathbf{x}_{red}$ gives the reduced state vector containing the tropospheric and stratospheric column. Here $\mathbf{x}$ is the vector containing the ozone amounts in Dobson units for the individual layers of the atmosphere, starting with the layer at the top of the atmosphere. Assuming that p_T lies between the pressure levels p_k and p_{k+1} the matrix $\mathbf{W}$ will have the following shape

$$\mathbf{W} = \begin{pmatrix} 0 & 0 & \ldots & 0 & (p_k - p_T)/(p_k - p_{k+1}) & 1 & \ldots & 1 & 1 & 1 \\ 1 & 1 & \ldots & 1 & (p_T - p_{k+1})/(p_k - p_{k+1}) & 0 & \ldots & 0 & 0 & 0 \end{pmatrix}$$

The tropospheric and stratospheric columns follow from $\mathbf{x}_{red} = \mathbf{Wx}$, the error covariance matrix follows from $\mathbf{S}_{red} = \mathbf{WSW}^T$, where $\mathbf{W}^T$ is the transpose of $\mathbf{W}$, and the averaging kernel follows from $\mathbf{A}_{red} = \mathbf{WAW}^T (\mathbf{WW}^T)^{-1}$.

Appendix B: Converting Partial Columns to Volume Mixing Ratio

The ozone concentration in the OMO3PR output files is in Dobson Units (DU) per layer. To convert these partial columns to the average mixing ratio, the following equation should be used:

$$<vmr>_i = c \frac{N_i}{dp_i} \, ,$$

where N_i is the partial column in DU, dp_i is the pressure difference between the bottom and top of the layer in hPa, c is a constant of 1.2672 and $<vmr>_i$ is the average volume mixing ratio in ppmv.

The averaging kernel can be expressed for the ozone profiles in volume mixing ratio as:

$$A_{ij}^{vmr} = A_{ij}^{DU} \frac{dp_j}{dp_i} \, ,$$

where A^{vmr} is the averaging kernel for the profiles in vmr and A^{DU} for the profiles in DU.